ACS Chemical Neuroscience

Letter

pubs.acs.org/chemneuro

MRI Sensing of Neurotransmitters with a Crown Ether Appended Gd^{3+} Complex

Fatima Oukhatar,[†,‡] Sandra Même,[†] William Même,[†] Frédéric Szeremeta,[†] Nikos K. Logothetis,[‡,§] Goran Angelovski,*[,∥] and Éva Tóth*[,†]

[†]Centre de Biophysique Moléculaire, CNRS, rue Charles Sadron, 45071 Orléans, Cedex 2, France

[‡]Department for Physiology of Cognitive Processes, Max Planck Institute for Biological Cybernetics, Tübingen 72076, Germany

[§]Department of Imaging Science and Biomedical Engineering, University of Manchester, Manchester M13 9PL, United Kingdom

[∥]MR Neuroimaging Agents Group, Max Planck Institute for Biological Cybernetics, Spemannstr. 41, 72076 Tübingen, Germany

S *Supporting Information*

ABSTRACT: Molecular magnetic resonance imaging (MRI) approaches that detect biomarkers associated with neural activity would allow more direct observation of brain function than current functional MRI based on blood-oxygen-level-dependent contrast. Our objective was to create a synthetic molecular platform with appropriate recognition moieties for zwitterionic neurotransmitters that generate an MR signal change upon neurotransmitter binding. The gadolinium complex (**GdL**) we report offers ditopic binding for zwitterionic amino acid neurotransmitters, via interactions (i) between the positively charged and coordinatively unsaturated metal center and the carboxylate function and (ii) between a triazacrown ether and the amine group of the neurotransmitters. **GdL** discriminates zwitterionic neurotransmitters from monoamines. Neurotransmitter binding leads to a remarkable relaxivity change, related to a decrease in hydration number. **GdL** was successfully used to monitor neural activity in ex vivo mouse brain slices by MRI.

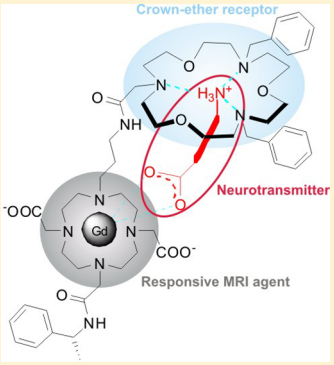

KEYWORDS: *Crown ether, gadolinium, MRI, neurotransmitter sensing, responsive agent*

Cognitive capacities of our brains reflect the activity of self-organizing complex dynamic networks, characterized by massive, differentiated neuronal connectivity. The complexity of the latter is largely due to the strong chemical differentiation of synapses. Synaptic chemistry involves cascades of dynamic changes of a multitude of molecules and ions. The study of dynamic and effective connectivity of such networks requires combination of methodologies, including invasive neurophysiological measurements and global neuroimaging. Today, magnetic resonance imaging (MRI) is indeed extensively used in studying brain function as well as in the diagnosis of neurological disorders.[1] A functional variant of MRI, based on blood-oxygen-level-dependent (BOLD) contrast is the mainstay of current neuroimaging. BOLD-fMRI has great potential but also serious limitations, as it measures surrogate signals, for example, hemodynamic responses, and reflects neuronal mass activity.[2] To go beyond BOLD MRI, functional molecular imaging approaches have to be developed that allow more direct observation of neural activity via the detection of biomarkers associated with neural functioning.[3,4] Ideally, one would need chemical sensors that are small (recording at the level of synapses), fast (at the time scale of release/uptake), chemically selective, and selectively and simultaneously report on different neurotransmitters.[5] Moreover, in order to be able to map the entire brain, the performance of the detection technique should not depend on depth or simply tissue thickness. This approach too makes MRI the method of choice, provided chemical sensors are available. Many molecular probes for magnetic resonance neuroimaging were designed to detect calcium concentration changes,[6] either in the intracellular[7] or in the extracellular range.[8−10] Apart from calcium, neurotransmitters play a key role in signal transduction, but the noninvasive in vivo monitoring of their concentration changes by imaging techniques remains a challenge.[11] Recently, the chemical exchange saturation transfer (CEST) effect of the glutamate amine protons was proposed to image glutamate in rat and human brain.[12] In vivo magnetic resonance spectroscopy can also report on average glutamate or GABA (γ-amino butyric acid) concentrations in the brain; however, the time scale and the resolution of spectroscopic studies are inappropriate for monitoring the dynamics of neural activation. Contrary to Ca^{2+} detection, much less effort has been dedicated to neurotransmitter sensing with responsive MRI probes. The Jasanoff group reported paramagnetic heme-containing proteins engineered to have high affinity for dopamine instead of arachidonic acid.[13,14] In vivo experiments in rats demonstrated the potential of this approach to monitor extracellular dopamine levels, and for time-resolved volumetric measurements of dopamine-release evoked by reward-related brain stimulation.[15] Parker et al. reported Gd^{3+} complexes containing binding moieties targeted to metabotropic glutamate- or *N*-

Published: December 11, 2014

   dx.doi.org/10.1021/cn500289y | *ACS Chem. Neurosci.* 2015, 6, 219−225

methyl-D-aspartate (NMDA) receptors.[16,17] Yet, to the best of our knowledge, no responsive Gd^{3+}-based MRI agents have been reported so far with a binding site for neurotransmitters.

Our objective was thus to create a synthetic molecular platform, smaller than the robust proteins, with appropriate recognition moieties for neurotransmitters that generate an MR signal change upon neurotransmitter binding. Based on their size, neurotransmitters can be broadly split into two major groups: relatively large neuroactive peptides and small-molecule neurotransmitters. The latter include acetylcholine, biogenic amines (dopamine, noradrenaline, serotonin, and histamine), and amino acid neurotransmitters (GABA, glutamate, aspartate, and glycine). By far, the most prevalent transmitter is glutamate (millimolar concentration range), which is excitatory at well over 90% of the synapses in the human brain. The second most prevalent neurotransmitter is GABA, the major inhibitory neurotransmitter. Our choice was to target zwitterionic amino acid neurotransmitters without necessarily seeking for selectivity to individual neurotransmitters in a first approach. The aim of this first study has been to effectively track brain activity by MRI contrast changes induced by the cumulative effect of concentration variation in several neurotransmitters.

Zwitterionic amino acid neurotransmitters can be considered as bifunctional guests, thus receptors should have two binding sites adapted for NH_3^+ and COO^- groups, placed at an appropriate distance. Multivalent interactions are known to be more potent and selective over monovalent ones and contribute to increased association strength of the host−guest complex.[18,19] Our design concept therefore involved interactions (i) between a positively charged and coordinatively unsaturated Gd^{3+} chelate and the carboxylate function of the neurotransmitters and (ii) between a triazacrown ether appended on the chelate and the amine group of the neurotransmitters. In order to achieve a positive overall charge of the metal chelate, we have chosen an amide derivative of DO3A for Gd^{3+} coordination. For the crown ether, a derivative of 18⟨$O_3N_3$2$_6$corand-6⟩ was selected,[20] since the arrangement of the three nitrogen atoms matches the symmetry axis of a primary ammonium cation thus enabling the formation of three strong N···H−N hydrogen bonds.[21] This increases selectivity for NH_4^+ over K^+. Although many different hosts have been described for amine binding,[22] the relative synthetic simplicity associated with azacrown ethers and their conjugation to a Gd^{3+} complex was an important parameter. Upon neurotransmitter binding to this probe, the coordinated water is expected to be expelled by the carboxylate of the neurotransmitter, resulting in a relaxivity decrease ("turn-off" response; Figure 1). Due to the difficulties associated with brain delivery of molecules larger than ∼600 Da, these agents would rather be administered via intracranial injection for in vivo animal experiments.[15]

The substituted triaza crown ether was prepared by partially following the synthetic procedure previously reported for oligonucleotide crown ether conjugates.[23] The synthesis commenced from a commercially available 2-(2-aminoethoxy)-ethanol which was treated with benzoic anhydride and subsequently mesylated to give building block **2** (Figure 2). Its treatment with ethanolamine afforded dibenzoyl diamide **3**, which was reduced with $LiAlH_4$ to the corresponding diamine **4**. The first aza-crown ether **5** was formed by intermolecular cyclization of **4** with diglycolyl chloride. This was treated with $LiAlH_4$ to reduce the two amides of **5** into amines in **6**. Finally, the Jones oxidation of the alcohol group in **6** yielded the desired building block, the carboxylic acid **7** which was used for

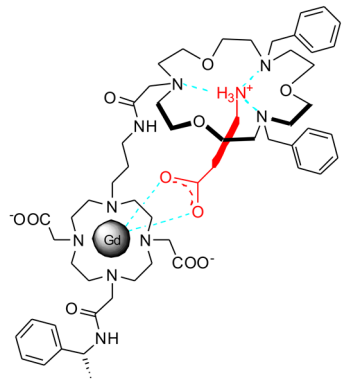

Figure 1. GdL, an MRI probe designed for sensing zwitterionic amino acid neurotransmitters (in red) via potentially ditopic host−guest interaction.

coupling with the macrocyclic Gd^{3+} chelator. For this, we first alkylated DO2A-*t*-Bu ester with the bromide **8** to obtain **9**, a monoamide derivative of DO3A. Reductive amination of this molecule with 3-[(benzyloxycarbonyl)amino]-propionaldehyde in the presence of $Na(OAc)_3BH$ yielded **10**. A reductive cleavage of the Cbz protected amine provided primary amine **11** which was condensed with the azacrown **7** and treated with formic acid to afford the Gd^{3+} chelator **L** appended with the crown-ether. Complexation of **L** with Gd^{3+} yielded the desired complex **GdL**.

Neurotransmitter binding was investigated by monitoring the variation of the longitudinal water proton relaxivity, r_1, of **GdL** upon addition of the nonzwitterionic acetylcholine and different zwitterionic amino acid neurotransmitters (aspartate, GABA, glutamate or glycine). **GdL** exhibits a strong relaxivity decrease upon binding of the zwitterionic glutamate, aspartate and glycine, and to a lower extent in the presence of GABA (Figure 3). Serotonin and noradrenaline have negligible effect (not shown). The relaxivity decrease observed upon acetylcholine addition is much smaller than that with amino acids, obviously due to the absence of a carboxylic group and to the lower affinity of the trimethylammonium group toward the azacrown host.[22] The effect of bicarbonate and phosphate was also investigated since these are two significant and often interfering components of physiological fluids. Bicarbonate is the most abundant extracellular anion (∼25 mM), compared to ∼1 mM concentration of hydrogen phosphate.[24] So far, it is not known if bicarbonate concentrations change in the brain during neuronal activity. **GdL** displays a relaxivity decrease upon bicarbonate titration in a similar extent as with the zwitterionic neurotransmitters (Figure 3). On the other hand, a limited relaxivity change (18%) is observed upon addition of 100 equiv of phosphate (not shown). Upon addition of 100 equiv of KCl, no relaxivity decrease is observed evidencing that chloride ions are not competitors.

The relaxometric titration curves were fitted to calculate affinity constants for the ternary complexes (K_a = [**GdL**-A]/[**GdL**][A], where A stands for the neurotransmitter or anion; Table 1). The affinity constants show selectivity of **GdL** for α-amino acids (glycine, aspartate, and L-glutamate) over the γ-amino acid GABA. For instance, synaptically released glutamate is estimated to reach a concentration of few millimolar.[25] Hence, the affinity constant determined for **GdL** is well adapted to detection in this concentration range. On the other hand, the larger size of GABA seems less suited for dual binding that

dx.doi.org/10.1021/cn500289y | ACS Chem. Neurosci. 2015, 6, 219−225

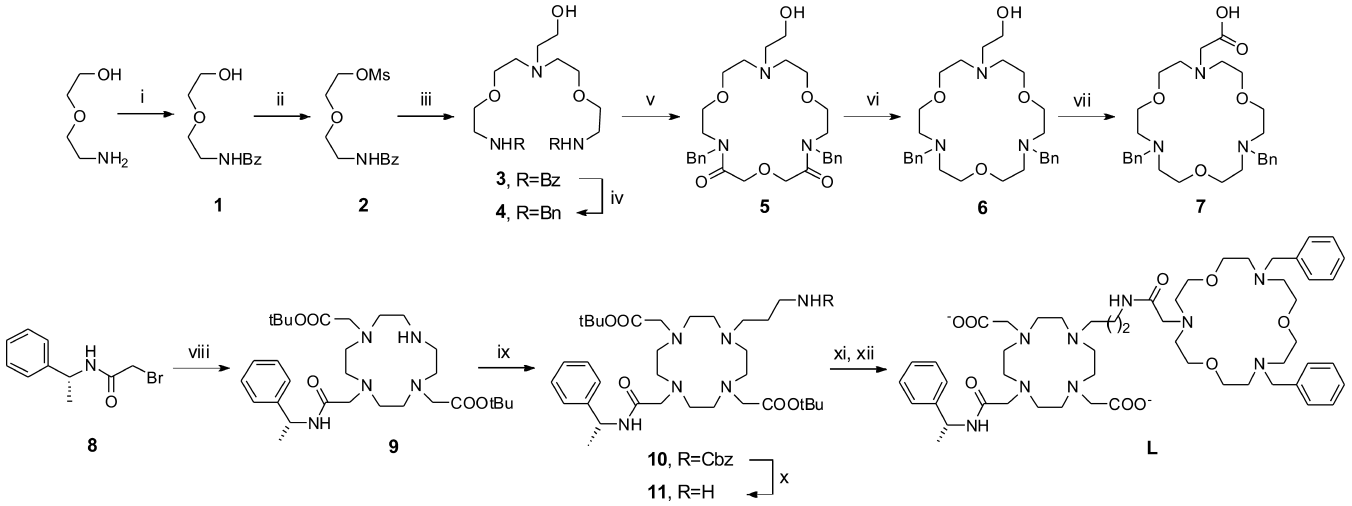

Figure 2. Synthesis of the ligand **L**. Reagents, conditions, and isolated yields: (i) benzoic anhydride, EtOH, reflux, 86%; (ii) CH_3SO_2Cl, NEt_3, 0 °C, CH_2Cl_2, 90%; (iii) ethanolamine, NEt_3, CH_3CN, reflux, 80%; (iv) $LiAlH_4$, THF, reflux, 81%; (v) diglycolyl chloride, NEt_3, 0 °C, CH_2Cl_2; (vi) $LiAlH_4$, THF, reflux, 61% (over two steps); (vii) CrO_3, H_2SO_4, acetone, 51%; (viii) DO2A-*t*-Bu ester, K_2CO_3, CH_3CN, 60 °C, 89%; (ix) $OHCCH_2CH_2NHCbz$, $Na(OAc)_3BH$, THF, rt, 75%; (x) H_2, Pd/C, EtOH, 90%; (xi) 7, HBTU, DMF, rt; (xii) HCOOH, 60 °C, 58% (over two steps).

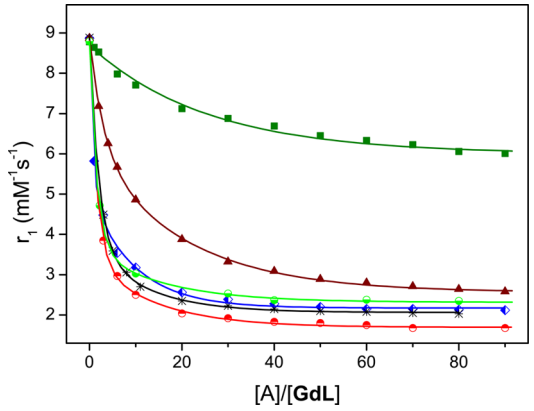

Figure 3. ^1H NMR relaxometric titrations of **GdL** (2 mM) with different neurotransmitters and anions (A) at 37 °C and pH 7.4 (HEPES 25 mM) and 300 MHz. The r_1 changes are presented for acetylcholine (solid dark green square, dark green line), GABA (solid brown up triangle, brown line), hydrogen carbonate (open green circle, green line), aspartate (open blue tilted square, blue line), glutamate (black asterisk, black line) and glycine (open red circle, red line). The lines represent the fit as explained in the text.

Table 1. Affinity Constants and Maximum Relaxivity Changes upon Interaction with Neurotransmitters and Small Anions

A	K_a (M^{-1})	$-\Delta r_1$ (%)[a]
acetylcholine		32
GABA	99 (8)	72
hydrogencarbonate	440 (10)	74
aspartate	345 (20)	76
glutamate	312 (20)	77
glycine	345(15)	81

[a] $-\Delta r_1 = 100\text{-}(r_{1,A}:r_{1,init}) \times 100$, where $r_{1,init}$ is the initial relaxivity and $r_{1,A}$ is the relaxivity at the end of the titration.

involves both the metal center and the crown ether. This consequently suggests that the crown ether is participating in the binding.

Considering the effect of bicarbonate, we can reasonably assume that the binding also involves the CO_3^{2-} ion, as it was previously stated.[26] The binding affinity of the dinegative anion will be higher than that of the carboxylate of the amino acid bearing a single negative charge. Steric effects might be also important: even at equal charge, the binding is likely stronger for the small-size bicarbonate than for a larger-size amino acid. Unfortunately, these differences are not overcome to a large extent by the contribution of the interaction between the amine of the neurotransmitter and the crown ether and the overall result is a similar binding affinity for bicarbonate and neurotransmitter molecules.

In order to better discriminate zwitterionic neurotransmitters with respect to carbonate, one should increase the contribution of the amine binding to the overall affinity (i) by diminishing the relative importance of carboxylate binding and (ii) by increasing the amine binding strength. The two strategies can be pursued in parallel. The first aspect can be achieved by decreasing the positive charge of the **GdL** complex. To increase the amine binding affinity, the crown ether moiety can be replaced by other amine receptors. Although a wide variety of synthetic hosts for amines has been described to date, many of them are synthetically not easily accessible and not available to conjugation to a metal chelating unit (e.g., calixarenes, resorcin[4]arenes, cucurbiturils, metal porphyrin complexes, etc.).[22] A more adapted amine recognition unit can be the *m*-xylene bisphosphonate moiety which has been described by Schrader.[27]

Luminescence lifetime measurements on the Eu^{3+} analogue **EuL** in the absence and in the presence of 50 equiv of glutamate evidenced the decrease of the hydration number from 1.2 to 0.4 upon neurotransmitter binding. Monohydration of the **GdL** complex has been also confirmed by ^{17}O NMR; the chemical shifts unambiguously prove one inner sphere water molecule (Supporting Information). In the absence of neurotransmitters, the LnL complex is expected to be nine-coordinate, involving also the coordination of the amide oxygen of the $-(CH_2)_n-NHCO-$ linker as it was proved by infrared spectra for structurally analogue DO3A derivatives.[28]

dx.doi.org/10.1021/cn500289y | ACS Chem. Neurosci. 2015, 6, 219−225

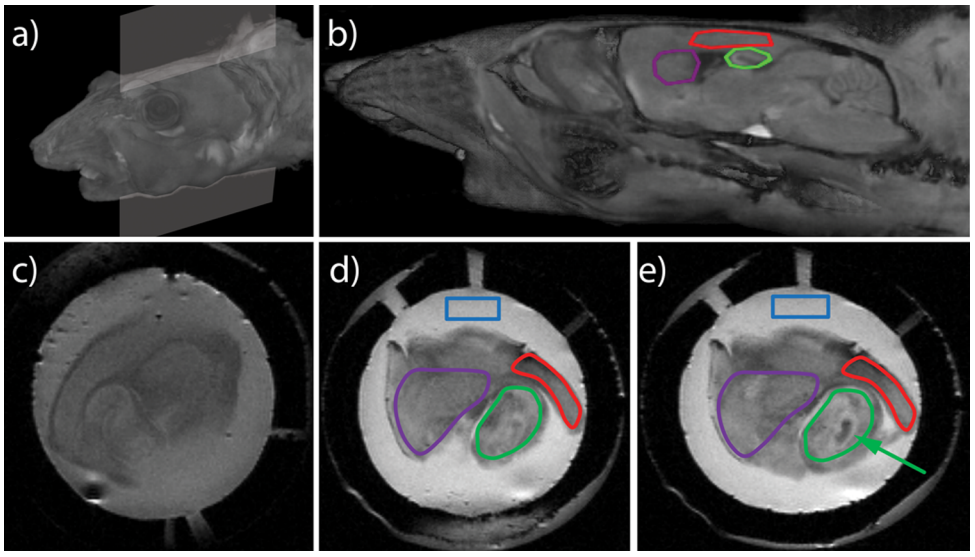

Figure 4. Reconstituted 3D MR image of a mouse head showing (a) the orientation of the examined slice and (b) the brain structures with the ROIs. MR image of a mouse brain slice in the absence (c) and in the presence of 500 μM **GdL** with the ROIs indicated (d): medium (blue), striatum (purple), cortex (red), and hippocampus (green). MR image of the same slice 10 min after KCl addition (e). The highest signal intensity decrease is observed in the center of the hippocampus (indicated with the arrow).

In contrast to typical monohydrated, nine-coordinate DOTA-type chelates which do not form ternary complexes at physiological pH,[29] **GdL** is able to act as a responsive probe to neurotransmitters by accommodating carboxylate donors, thanks to the positive charge of the chelate and the weak binding of the linker amide.

Relaxometric titrations were performed under the same conditions (37 °C, pH 7.4, 300 MHz) with glutamate and glycine on the bishydrated GdDO3A, well-known to bind small anions.[26] Roughly twice weaker maximum r_1 changes (40% and 32%) and much lower affinity constants (K_a = 25 and 15 M^{-1} for glycine and glutamate, respectively) were observed with respect to **GdL** (Supporting Information). These results underline the importance of the ditopic recognition unit and the positive charge in **GdL** as design elements to create a neurotransmitter-sensitive MRI agent.

It should be noted that the initial relaxivity of **GdL** (8.8 mM^{-1} s^{-1} at 37 °C, 300 MHz) is high for a monohydrated chelate. This is explained in terms of (i) a second sphere relaxation effect promoted by the water molecules around the triazacrown, and (ii) a slow rotational motion of the complex due to the bulkiness of the crown ether with the pending benzyl groups. Slow rotation was evidenced by the rotational correlation time calculated from ^{17}O longitudinal relaxation rates which is almost 5 times as high as that for GdDOTA (τ_R^{298} = 360 ps for **GdL** vs 77 ps for GdDOTA, Supporting Information).

The water exchange rate on **GdL**, obtained from the ^{17}O NMR data (Supporting Information), is $k_{ex}^{298} = 1.35 \times 10^7$ s^{-1}, about three times higher than that on $[Gd(DOTA)(H_2O)]^-$. This is interesting since the replacement of carboxylate functions with amides typically slows down the water exchange. However, the two amide functions in **GdL** are very different from each other. The coordination of the amide oxygen in the $-CH_2CH_2NHCO-$ moiety closer to the crown ether induces a strong steric crowding by forming a seven-membered chelate ring which results in an important acceleration of the water exchange, as it was previously observed,[28] thus largely compensating the decrease in the water exchange rate due to the $-CH_2CONH-$ moiety.

In order to provide a proof of concept that our probe is capable of reporting on neurotransmitter concentration changes under biologically relevant conditions, MRI experiments have been carried out on acute mouse brain slices following neuronal stimulation. Swiss mice (female, 5−6 weeks old) were euthanized by decapitation and 500 μm thick sagittal brain slices were prepared and immerged in 500 μL of artificial cerebrospinal fluid (124 mM NaCl, 3 mM KCl, 3 mM $MgCl_2$, 3 mM $CaCl_2$, 1.3 mM NaH_2PO_4, 10 mM dextrose, 10 mM HEPES) in the absence or presence of 0.5 mM **GdL** (Figure 4). In this proof of principle study, we used an artificial cerebrospinal fluid which contains HEPES buffer instead of carbonate,[30,31] in order to avoid saturation of our imaging agent by carbonate binding. MRI experiments were performed at 7 T using a homemade loop gap coil specifically developed for the purpose of imaging mouse brain slices. In order to provoke intense neuronal activity, KCl (40 mM) was added to the medium and sequential imaging was performed for 12 min (the viability of the brain slices might decline afterward). KCl induces membrane potential depolarization and neuronal activity, followed by neurotransmitter release. Mean gray levels were measured every 2 min in five regions of interest (ROIs): in the cortex, the striatum, the hippocampus, the center of the hippocampus, and in the medium itself. In the presence of 500 μM **GdL**, the intensity is higher not only in the medium, but also in brain tissues, suggesting good diffusion of the probe into the parenchyma. Without stimulation with KCl, the MR signal intensity in all ROIs is stable over time both in the absence or presence of the contrast agent.

Upon KCl addition, signal intensity was consistently found to decrease in the cortex, the striatum, and the hippocampus, while no significant change was observed in the medium. The most important signal intensity-decrease occurred in the hippocampus, in accordance with the significant neurotransmitter release expected in this region, whereas the signal change was delayed and less marked in the cortex and striatum (Figure 5a). The signal intensity decrease was particularly

dx.doi.org/10.1021/cn500289y | ACS Chem. Neurosci. 2015, 6, 219−225

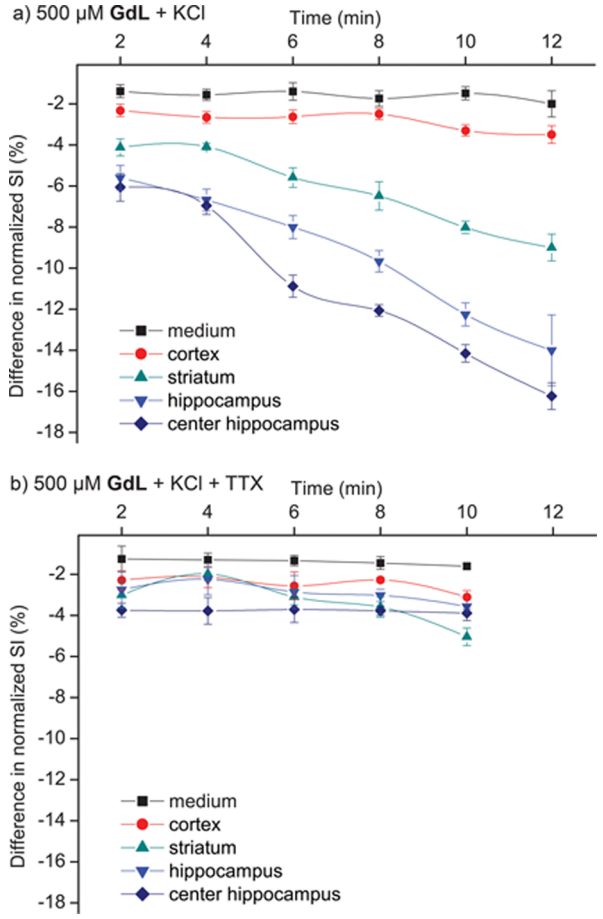

Figure 5. Time course of normalized signal intensity (SI) variation (in %) in different ROIs (medium, cortex, striatum, hippocampus, and center of hippocampus) of mouse brain slices with respect to the first image taken immediately after addition of 40 mM KCl to the medium in the absence (a) and in the presence (b) of tetrodotoxin. The data correspond to average intensity variations observed in $n = 6$ slices (from three mouse brains) for (a) and $n = 4$ for (b). The lines connecting SI values within the same ROI serve to guide eyes.

important in the central structure of the hippocampus which can be likely identified as the CA1 field. CA1 pyramidal cells receive strong input both from the CA3 neurons via the Schaffer Collateral Pathway and directly from the Perforant Path. Release of glutamate at these synapses activates NMDA- and AMPA-type ionotropic glutamate receptors localized at dendritic spines of CA1 pyramids.[32] It has been recently shown that epileptiform discharges induced by high-K^+ are predominantly initiated from the stratum pyramidale layer of CA3 and propagated to CA1.[33] These findings suggest that synaptic release of glutamate can be more marked in the CA3−CA1 fields than in other hippocampal structures; therefore, we hypothesize that the most significant signal decrease in the center of the hippocampus observed in our experiments corresponds to this region. When repeating the same experiment without **GdL** or with GdDOTA instead of **GdL**, no signal intensity change is detected in any of the ROIs (Supporting Information). The signal intensity decrease observed in the presence of **GdL** is attributed to the decreasing relaxivity of the agent on neurotransmitter binding (Figure 3). The continuous signal intensity decrease shown in Figure 5a is related to the continuous release of neurotransmitters upon KCl stimulation over time. The contrast agent is present in excess and will likely capture the zwitterionic neurotransmitters released over time.

Similar experiments were performed on brain slices pretreated with the sodium channel antagonist tetrodotoxin (TTX, 10 μM, Figure 5b). TTX inhibits voltage-gated Na^+ channels[34] and the generation of action potential which is required for stimulus-evoked neurotransmitter release in most neurons. The results show that, following TTX pretreatment, KCl did not induce signal change in any brain structure. When considering the action of high K^+ concentrations, two mechanisms have to be taken into account. The first involves an increase in neuronal firing (bursts of action potential) and neurotransmission. Neuronal firing is blocked by TTX. In the second mechanism, which is TTX-resistant,[35] synaptic terminals are depolarized and influx of calcium ions by voltage-sensitive calcium channels in the terminal membrane will increase the release of neurotransmitters. The fact that in the presence of TTX the signal intensity change is strongly reduced suggests that, under our experimental conditions, the main source of neurotransmitter release upon KCl stimulation is neuronal firing and neurotransmission. Although we cannot exclude neurotransmitter release by depolarization of synaptic terminals, this contribution is less important.

In conclusion, we have synthesized a Gd^{3+}-based MRI agent with a relaxometric response to amino acid neurotransmitters. The chemical design offers ditopic binding via interactions between a positively charged metal complex and the carboxylate and between the crown ether moiety and the amine of amino acids. The probe shows selectivity toward zwitterionic over nonzwitterionic neurotransmitters. Neurotransmitter binding leads to a remarkable relaxivity decrease, due to a decrease in the hydration number. **GdL** was successfully used to monitor neural activity in acute mouse brain slices by MRI. The intensity decrease detected, in particular in the hippocampus, upon KCl stimulation results from the cumulative effect of various zwitterionic neurotransmitters. Although further improvement is needed in the chemical design to achieve selectivity over carbonate by strengthening neurotransmitter binding via the amine function, this proof-of-concept study shows that Gd^{3+}-based responsive MRI probes can provide an alternative toward monitoring brain function under biologically relevant conditions.

METHODS

Ligand Synthesis. The experimental procedures to prepare **GdL** are provided in the Supporting Information.

Luminescence Lifetime Experiments. The lifetime measurements were performed on a QuantaMasterTM 3 PH fluorescence spectrometer from Photon Technology International, Inc. The measurements were performed in H_2O and D_2O (25 °C, pH 7.4, HEPES) at 5 mM **EuL** concentration. Excitation and emission slits were set to 2 nm. Each reported luminescence lifetime (Table S1) is the average of 3 values involving 25 scans (decay data) and the curves were fitted to first order exponential decays. The hydration number was calculated according to the following equation, where x in eq 1 takes into account the effect of exchangeable amide N−H oscillators:[36,37]

$$q_{Eu} = 1.2[(k_{H_2O} - k_{D_2O}) - 0.25 - 0.075x] \quad (1)$$

^{17}O NMR Experiments. Variable temperature transverse and longitudinal ^{17}O relaxation rates and chemical shifts have been measured on **GdL** in order to assess water exchange and rotational dynamics. Variable temperature ^{17}O NMR measurements on an aqueous solution of **GdL** were obtained on a Bruker Avance 500

dx.doi.org/10.1021/cn500289y | ACS Chem. Neurosci. 2015, 6, 219−225

(11.75 T, 67.8 MHz) spectrometer. The temperature was calculated according to a previous calibration with ethylene glycol and MeOH.[38] Acidified water ($HClO_4$, pH ∼ 4) was used as an external reference. Longitudinal ^{17}O relaxation times T_1 were measured by the inversion−recovery pulse sequence, and the transverse relaxation times T_2 were obtained by the Carr−Purcell−Meiboom−Gill spin−echo technique. To eliminate the susceptibility corrections to the chemical shift,[39] the samples were placed in a glass sphere fixed in a 10 mm NMR tube. For sufficient accuracy, samples with at least a 20 mM concentration of the **GdL** were used. To improve sensitivity, the amount of ^{17}O was enriched by adding $H_2{}^{17}O$ (10% $H_2{}^{17}O$, CortecNet) to achieve approximately 1% ^{17}O content in the sample. The least-squares fit of the data were performed by using Micromath Scientist version 2.0 (Salt Lake City, UT). Further details are provided in the Supporting Information.

Neurotransmitter Binding Studies. Ternary complex formation between **GdL** (or GdDO3A, data shown in Figure S2) and neurotransmitters was assessed by performing relaxometric titrations at 37 °C on a Bruker AvanceIII 300 MHz (7.05 T) spectrometer. The pH was maintained at 7.4 by using 25 mM HEPES buffer. A HEPES buffered solution of the neurotransmitter was added stepwise to 1 mM **GdL** complex solution. The affinity constants, $K_a = 1/K_d$, were determined according to the following equations where the paramagnetic relaxation rate $1/T_{1para}$ is the sum of the contributions originating from the free **GdL** complex and the **GdL**-analyte adduct (**GdL**-A). The $1/T_{1para}$ values measured as a function of the analyte (neurotransmitter) concentrations have been fitted to eq 2, where r_{1GdL} and r_{1GdLA} are the relaxivities of the free complex and the fully bound complex, respectively, K_a is the affinity constant, c_{GdL} and c_A represent the concentrations of **GdL** and analyte, respectively. K_a and r_{1GdLA} have been obtained through a two parameter fitting of the relaxation rate data measured at various analyte concentrations.

$$1/T_{1para} = (r_1^{GdL\text{-}A}Z + (c_{GdL} - Z)r_1^{GdL}) \times 1000,$$
$$\text{where } z = \frac{(K_d + c_{GdL} + c_A) + \sqrt{(K_d + c_{GdL} + c_A)^2 - 4(c_A \times c_{GdL})}}{2} \quad (2)$$

MRI Experiments with Brain Slices. Acute brain slices were prepared from Swiss mice (female, 5−6 weeks old). Animals were euthanized by decapitation, and brains were immediately removed and placed in cold artificial cerebrospinal fluid (aCSF) gassed with 95% O_2 and 5% CO_2 at 4 °C. Sagittal brain slices (500 μm thick) were cut using a vibratome (HM650 V, Microm Microtech, Francheville, France). Slices were subsequently incubated for 45−60 min at room temperature (22−24 °C), in gassed aCFS solution, containing 124 mM NaCl, 3 mM KCl, 3 mM $MgCl_2$, 3 mM $CaCl_2$, 1.3 mM NaH_2PO_4, 10 mM dextrose, and 10 mM HEPES (pH 7.3−7.4).

Brain slices were transferred into a 12 mm tube and placed between two adjacent horizontal inserts. Circular inserts consisted of nylon mesh to support and maintain tissue. Tubes were put in a homemade loop gap coil (14 mm diameter, 4 mm height) specifically developed for the purpose of imaging mouse brain slices. Acquisitions were performed on a 7 T horizontal magnet (Pharmascan 70/16 US, Bruker, Wissembourg) equipped with a 300 mT/m gradient set. A Bruker RARE8 sequence was performed every 2 min with the following parameters: TE/TR = 46.5 ms/2s, FOV = 2 cm × 2 cm, matrix size = 256 × 256 providing 80 μm × 80 μm × 150 μm images for an acquisition time of 2 min.

Brain slices were immerged in aCSF solution in the absence or presence of 500 μM **GdL**. In order to provoke neuronal activity and neurotransmitter release, 40 mM KCl (from a 4 M stock solution in aCSF) was added to the medium and sequential imaging was performed for a maximum of 16 min (Figure S4). In some experiments, brain slices were pretreated with the sodium channel antagonist tetrodotoxin (TTX) 10 μM, before being exposed to KCl.

ROIs were chosen in cortex, medium (with contrast agent), striatum, and hippocampus. Mean gray levels were measured in these four ROIs after each sequence (every 2 min) and then normalized to an ROI taken outside the tube sample holder. The difference in gray level intensity was calculated between the images in each ROIs. Image 1 was set as a reference, and all subsequent images were compared to this one. We could not take an image at 0 min (before KCl injection) as reference, since the slice slightly moved in the experimental chamber when KCl was added to the medium. Further details are provided in the Supporting Information.

■ ASSOCIATED CONTENT

Supporting Information

Synthetic procedures, additional experimental results and comments from luminescence lifetime measurements, ^{17}O NMR measurements, neurotransmitter binding studies and MRI experiments with brain slices. This material is available free of charge via the Internet at http://pubs.acs.org/.

■ AUTHOR INFORMATION

Corresponding Authors

*(G.A.) Fax: +49 7071 601 919. E-mail: goran.angelovski@tuebingen.mpg.de.

*(E.T.) Fax: +33 2 38 63 15 17. E-mail: eva.jakabtoth@cnrs-orleans.fr.

Author Contributions

G.A. and E.T. designed research; F. O. prepared the studied contrast agent and performed NMR and luminescence lifetime experiments; S. M., W. M., and F. S. performed and analyzed MRI brain slice experiments; N. K. L. supported research; all authors wrote the manuscript.

Funding

This work was supported by the CNRS, the Max-Planck Society, and the German Research Foundation (DFG, Grant AN 716/2-1).

Notes

The authors declare no competing financial interest.

■ ACKNOWLEDGMENTS

This work was carried out in the frame of COST TD1004 Action "Theranostics Imaging and Therapy".

■ REFERENCES

(1) Buxton, R. B. (2009) *Introduction to functional magnetic resonance imaging: principles and techniques*, 2nd ed., Cambridge University Press, Cambridge.

(2) Logothetis, N. K. (2008) What we can do and what we cannot do with fMRI. *Nature 453*, 869−878.

(3) Jasanoff, A. (2005) Functional MRI using molecular imaging agents. *Trends Neurosci. 28*, 120−126.

(4) Koretsky, A. P. (2012) Is there a path beyond BOLD? Molecular imaging of brain function. *NeuroImage 62*, 1208−1215.

(5) Andrews, A. M. (2013) The BRAIN Initiative: Toward a Chemical Connectome. *ACS Chem. Neurosci. 4*, 645−645.

(6) Bonnet, C. S., Tei, L., Botta, M., and Tóth, É. (2013) Responsive Probes, In *The Chemistry of Contrast Agents in Medical Magnetic Resonance Imaging*, pp 343−385, John Wiley & Sons, Ltd., New York.

(7) Li, W. H., Fraser, S. E., and Meade, T. J. (1999) A calcium-sensitive magnetic resonance imaging contrast agent. *J. Am. Chem. Soc. 121*, 1413−1414.

(8) Angelovski, G., Fouskova, P., Mamedov, I., Canals, S., Toth, E., and Logothetis, N. K. (2008) Smart magnetic resonance imaging agents that sense extracellular calcium fluctuations. *ChemBioChem 9*, 1729−1734.

(9) Dhingra, K., Maier, M. E., Beyerlein, M., Angelovski, G., and Logothetis, N. K. (2008) Synthesis and characterization of a smart contrast agent sensitive to calcium. *Chem. Commun.*, 3444−3446.

(10) Angelovski, G., Chauvin, T., Pohmann, R., Logothetis, N. K., and Tóth, É. (2011) Calcium-Responsive Paramagnetic CEST Agents. *Bioorg. Med. Chem. 19*, 1097−1105.
(11) Shapiro, M. G., Atanasijevic, T., Faas, H., Westmeyer, G. G., and Jasanoff, A. (2006) Dynamic imaging with MRI contrast agents: quantitative considerations. *Magn. Reson. Imaging 24*, 449−462.
(12) Cai, K., Haris, M., Singh, A., Kogan, F., Greenberg, J. H., Hariharan, H., Detre, J. A., and Reddy, R. (2012) Magnetic resonance imaging of glutamate. *Nat. Med. 18*, 302−306.
(13) Shapiro, M. G., Westmeyer, G. G., Romero, P. A., Szablowski, J. O., Kuster, B., Shah, A., Otey, C. R., Langer, R., Arnold, F. H., and Jasanoff, A. (2010) Directed evolution of a magnetic resonance imaging contrast agent for noninvasive imaging of dopamine. *Nat. Biotechnol. 28*, 264−270.
(14) Brustad, E. M., Lelyveld, V. S., Snow, C. D., Crook, N., Jung, S. T., Martinez, F. M., Scholl, T. J., Jasanoff, A., and Arnold, F. H. (2012) Structure-Guided Directed Evolution of Highly Selective P450-Based Magnetic Resonance Imaging Sensors for Dopamine and Serotonin. *J. Mol. Biol. 422*, 245−262.
(15) Lee, T., Cai, L. X., Lelyveld, V. S., Hai, A., and Jasanoff, A. (2014) Molecular-Level Functional Magnetic Resonance Imaging of Dopaminergic Signaling. *Science 344*, 533−535.
(16) Mishra, A., Gottschalk, S., Engelmann, J., and Parker, D. (2012) Responsive imaging probes for metabotropic glutamate receptors. *Chem. Sci. 3*, 131−135.
(17) Sim, N., Gottschalk, S., Pal, R., Engelmann, J., Parker, D., and Mishra, A. (2013) Responsive MR-imaging probes for *N*-methyl-D-aspartate receptors and direct visualisation of the cell-surface receptors by optical microscopy. *Chem. Sci. 4*, 3148−3153.
(18) Mammen, M., Choi, S. K., and Whitesides, G. M. (1998) Polyvalent interactions in biological systems: Implications for design and use of multivalent ligands and inhibitors. *Angew. Chem., Int. Ed. 37*, 2755−2794.
(19) Chung, M.-K., Lee, S. J., Waters, M. L., and Gagne, M. R. (2012) Self-Assembled Multi-Component Catenanes: The Effect of Multivalency and Cooperativity on Structure and Stability. *J. Am. Chem. Soc. 134*, 11430−11443.
(20) Steed, J. W., and Atwood, J. L. (2009) *Supramolecular chemistry*, 2nd ed., Wiley, Oxford.
(21) Lehn, J. M., and Vierling, P. (1980) The [18]-N_3O_3 aza-oxa macrocycle: a selective receptor unit for primary ammonium cations. *Tetrahedron Lett. 21*, 1323−1326.
(22) Späth, A., and König, B. (2010) Molecular recognition of organic ammonium ions in solution using synthetic receptors. *Beilstein J. Org. Chem. 6*, 32.
(23) Vogel, S., Rohr, K., Dahl, O., and Wengel, J. (2003) A substituted triaza crown ether as a binding site in DNA conjugates. *Chem. Commun.*, 1006−1007.
(24) May, P. M., Linder, P. W., and Williams, D. R. (1977) Computer Simulation of Metal-ion Equilibria in Biofluids: Models for the Low-molecular-weight Complex Distribution of Calcium(II), Magnesium(II), Manganese(II), Iron(III), Copper(II), Zinc(II), and Lead(II) Ions in Human Blood Plasma. *J. Chem. Soc., Dalton Trans.*, 588−595.
(25) Budisantoso, T., Harada, H., Kamasawa, N., Fukazawa, Y., Shigemoto, R., and Matsui, K. (2013) Evaluation of glutamate concentration transient in the synaptic cleft of the rat calyx of Held. *J. Physiol. 591*, 219−239.
(26) Botta, M., Aime, S., Barge, A., Bobba, G., Dickins, R. S., Parker, D., and Terreno, E. (2003) Ternary complexes between cationic Gd^{III} chelates and anionic metabolites in aqueous solution: An NMR relaxometric study. *Chem.—Eur. J. 9*, 2102−2109.
(27) Schrader, T. (1998) Anomer-selective molecular recognition of free amino sugars with simple bisphosphonate receptor molecules. *J. Am. Chem. Soc. 120*, 11816−11817.
(28) Congreve, A., Parker, D., Gianolio, E., and Botta, M. (2004) Steric control of lanthanide hydration state: fast water exchange at gadolinium in a mono-amide "DOTA" complex. *Dalton Trans.*, 1441−1445.
(29) Burai, L., Hietapelto, V., Kiraly, R., Toth, E., and Brucher, E. (1997) Stability constants and ^1H relaxation effects of ternary complexes formed between Gd-DTPA, Gd-DTPA-BMA, Gd-DOTA, and Gd-EDTA and citrate, phosphate, and carbonate ions. *Magn. Reson. Med. 38*, 146−150.
(30) Drew, P. J., Shih, A. Y., Driscoll, J. D., Knutsen, P. M., Blinder, P., Davalos, D., Akassoglou, K., Tsai, P. S., and Kleinfeld, D. (2010) Chronic optical access through a polished and reinforced thinned skull. *Nat. Methods 7*, 981−984.
(31) Romo-Parra, H., Trevino, M., Heinemann, U., and Gutierrez, R. (2008) GABA actions in hippocampal area CA3 during postnatal development: Differential shift from depolarizing to hyperpolarizing in somatic and dendritic compartments. *J. Neurophysiol. 99*, 1523−1534.
(32) Collingridge, G. L., Kehl, S. J., and Mclennan, H. (1983) Excitatory Amino-Acids in Synaptic Transmission in the Schaffer Collateral Commissural Pathway of the Rat Hippocampus. *J. Physiol. 334*, 33−46.
(33) Liu, J. S., Li, J. B., Gong, X. W., Gong, H. Q., Zhang, P. M., Liang, P. J., and Lu, Q. C. (2013) Spatiotemporal dynamics of high-K^+-induced epileptiform discharges in hippocampal slice and the effects of valproate. *Neurosci. Bull. 29*, 28−36.
(34) Kao, C. Y. (1986) Structure-Activity Relations of Tetrodotoxin, Saxitoxin, and Analogues. *Ann. N.Y. Acad. Sci. 479*, 52−67.
(35) Freedman, S. B., Dawson, G., Villereal, M. L., and Miller, R. J. (1984) Identification and Characterization of Voltage-Sensitive Calcium Channels in Neuronal Clonal Cell-Lines. *J. Neurosci. 4*, 1453−1467.
(36) Beeby, A., Clarkson, I. M., Dickins, R. S., Faulkner, S., Parker, D., Royle, L., de Sousa, A. S., Williams, J. A. G., and Woods, M. (1999) Non-radiative deactivation of the excited states of europium, terbium and ytterbium complexes by proximate energy-matched OH, NH and CH oscillators: an improved luminescence method for establishing solution hydration states. *J. Chem. Soc., Perkin Trans. 2*, 493−503.
(37) Dickins, R. S., Parker, D., deSousa, A. S., and Williams, J. A. G. (1996) Closely diffusing O-H, amide N-H and methylene C-H oscillators quench the excited state of europium complexes in solution. *Chem. Commun.*, 697−698.
(38) Raiford, D. S., Fisk, C. L., and Becker, E. D. (1979) Calibration of Methanol and Ethylene-Glycol Nuclear Magnetic-Resonance Thermometers. *Anal. Chem. 51*, 2050−2051.
(39) Hugi, A. D., Helm, L., and Merbach, A. E. (1985) Water Exchange on Hexaaquavanadium(III): a Variable-Temperature and Variable-Pressure ^{17}O-NMR Study at 1.4 and 4.7 T. *Helv. Chim. Acta 68*, 508−521.